

GRANULAR DYNAMICS SIMULATION OF CLUSTER FORMATION IN RISER FLOW

B.P.B. Hoomans, J.A.M. Kuipers and W.P.M. van Swaaij

*Twente University of Technology
Department of Chemical Engineering,
P.O. Box 217, 7500 AE Enschede, the Netherlands*

Introduction

The occurrence of clusters is one of the most characteristic features of dense gas-solid flow in the riser section of a Circulating Fluidized Bed (CFB). The existence of such clusters has a profound influence on the performance of a CFB unit as a chemical reactor. It is therefore of great importance to gain more insight into this phenomenon. Although the existence of clusters (regions of locally higher solid fraction) in dense riser flow is well accepted in the chemical engineering community, a clear definition is still lacking (Chen, 1995). Clusters were observed experimentally by (among many others) Horio and Kuroki (1994) using a laser sheet technique. They found that the clusters had a characteristic parabolic shape. Tsuo and Gidaspow (1990) used a Two-Fluid approach with constant solids viscosity in order to simulate the riser section of a CFB. They reported the formation of cluster-like structures as well as the typical core-annulus flow structure where the average solids concentration is considerably higher near the wall. Other Two-Fluid approaches incorporating the kinetic theory of granular flow (Sinclair and Jackson (1990), Nieuwland *et al.* (1996)) did not focus particularly on cluster formation but more on the radial segregation of solids. This type of model possesses a peculiar dependency on the magnitude of the coefficient of restitution where a small deviation from unity causes the flow structure to change completely while the agreement with experimental findings deteriorates. This was (among others) pointed out by Hrenya and Sinclair (1997) who also reported that when particle phase turbulence was included this dependency became far less pronounced. Tanaka *et al.* (1996) performed simulations of gas-solid flow in a vertical duct using the Lagrangian approach for the solid particles. They employed the Direct Simulation Monte Carlo (DSMC) method to describe the particle dynamics. In this DSMC method the simulated particles actually represent a certain number of 'real' particles. A Monte Carlo procedure is invoked to determine the collision partners and the geometry of the collision. Hence this method does not account for actual particle-particle and particle-wall interaction in a direct way. Moreover the modified Nanbu method used in their work does not guarantee exact conservation of energy (Frezza, 1997) which can be an important drawback especially since the collision parameters turned out to be of key importance in their simulations. In this paper we present an extension of our Eulerian Lagrangian simulation technique (Hoomans *et al.* (1996)) for dense gas-solid two-phase flow in a riser which features a direct incorporation of the particle-particle and particle-wall interaction.

Granular Dynamics

In Granular Dynamics simulations the Newtonian equations of motion for each individual particle in the system are solved. We follow the hard-sphere approach which implies that the particles interact through binary, quasi-instantaneous, inelastic collisions with friction. Since most details of the model are presented in a previous paper (Hoomans *et al.* (1996)), the key features will be summarized briefly here. The collision model presented by Wang and Mason (1992) is used. The key parameters of the model are the coefficient of restitution ($0 \leq e \leq 1$) and the coefficient of friction ($\mu \geq 0$). In our approach a sequence of binary collisions is processed one collision at a time. This implies that a collision list is compiled in which for each particle a collision partner and a corresponding collision time is stored. A constant time step is used to take the external forces into account and *within* this time step the prevailing collisions are processed sequentially. In order to reduce the required CPU time neighborlists are used to limit the number of particles to be checked for possible collisions. Efficient algorithms obtained from the field of Molecular Dynamics (MD) are employed to achieve very efficient computational procedures.

External Forces

The equation of motion used in this work is:

$$m_p \frac{d\mathbf{v}_p}{dt} = m_p \mathbf{g} + \mathbf{F}_{drag} + \mathbf{F}_{LG} + \mathbf{F}_{LM} \quad (1)$$

where m_p represents the mass of a particle and \mathbf{v}_p its velocity. In Eq. (1) the first term on the right hand side is due to gravity and the second term is due to drag:

$$\mathbf{F}_{drag} = \frac{1}{8} \pi d_p^2 C_d \rho_g |\mathbf{u} - \mathbf{v}_p| (\mathbf{u} - \mathbf{v}_p) \mathcal{E}^{-2.7} \quad (2)$$

In Eq. (2) ρ_g represents the density of the gas phase and \mathbf{u} represents its velocity. It should be noted that the drag correction due to the presence of other particles has been accounted for via the well-known Richardson and Zaki (1954) correction factor. The drag coefficient for an isolated particle depends on the particle Reynolds number as given by Rowe and Henwood (1961):

$$C_d = \begin{cases} \frac{24}{\text{Re}_p} \left(1 + 0.15 (\text{Re}_p)^{0.687} \right) & \text{Re}_p < 1000 \\ 0.44 & \text{Re}_p \geq 1000 \end{cases} \quad (3)$$

where the particle Reynolds number is defined as:

$$\text{Re}_p = \frac{\varepsilon \rho_g |\mathbf{u} - \mathbf{v}_p| d_p}{\mu_g} \quad (4)$$

Gravity and drag force are implemented by default in all simulations shown in this work. The lift forces are used in one simulation in order to test their influence and will subsequently be discussed in more detail.

The second term on the right hand side of Eq. (1) is the lift force due to a velocity gradient. Following the lines of Tanaka *et al.* (1996) only the gradient in the x-direction is considered:

$$\mathbf{F}_{LG,x} = \frac{1}{8} \pi d_p^2 C_{LG} \rho_g |\mathbf{u} - \mathbf{v}_p|^2 \text{sign}(\chi) \quad (5)$$

where χ denotes the velocity gradient $\partial(u_y - v_{p,y})/\partial x$.

The empirical relations used for the lift coefficient C_{LG} are summarized in Table 1.

The third term on the right hand side in Eq. (1) is the lift force due to rotation, also known as Magnus lift force:

$$\mathbf{F}_{LM} = \frac{1}{8} \pi d_p^2 C_{LM} \rho_g |\mathbf{u} - \mathbf{v}_p| \frac{(\mathbf{u} - \mathbf{v}_p) \times \boldsymbol{\omega}_r}{|\boldsymbol{\omega}_r|} \quad (6)$$

where $\boldsymbol{\omega}_r$ is defined as follows:

$$\boldsymbol{\omega}_r = \boldsymbol{\omega} - \frac{1}{2} \nabla \times \mathbf{u} \quad (7)$$

The empirical relations used for the lift coefficient C_{LM} are summarized in Table 1.

The rotational velocity of particles is not only affected by collisions with the system walls or with other particles, but also by the torque exerted by the fluid:

$$I \frac{d\omega}{dt} = -\frac{1}{64} \pi d_p^5 C_m \rho_g |\omega_r| \omega_r \cdot \quad (8)$$

The empirical relations used for the lift coefficient C_m are summarized in Table 1.

Table 1, Empirical relations for the lift coefficients

$\frac{C_{LG}}{C_{LG,Sa}} = \left(1 - 0.3314 \xi^{1/2}\right) \exp\left(-\frac{Re_p}{10}\right) + 0.3314 \xi^{1/2} \quad Re_p \leq 40$		(Mei, 1992)
$\frac{C_{LG}}{C_{LG,Sa}} = 0.0741 Re_\chi^{1/2} \quad Re_p > 40$		
with: $C_{LG,Sa} = 8.225 \frac{Re_\chi^{1/2}}{Re}$ (Saffman, 1965), $\xi = \frac{d_p \chi }{2 \mathbf{u} - \mathbf{v}_p }$ and $Re_\chi = \frac{\rho_g \chi d_p^2}{4\mu_g}$		
$C_{LM} = 2\gamma \quad Re_p < 10$	with: $\gamma = \frac{d_p \omega_r }{2 \mathbf{u} - \mathbf{v}_p }$	
$C_{LM} = 3.8\gamma Re_p^{-1/2} \quad 10 < Re_p < 500$	(Oesterlé, 1994)	
$C_{LM} = 0.40\gamma \quad 500 < Re_p$	(Tsuji <i>et al.</i> , 1985)	
$C_m = \frac{1}{\pi} \left(\alpha Re_\omega^{-1/2} + \beta Re_\omega^{-1} \right)$		with: $Re_\omega = \frac{\rho_g \omega_r d_p^2}{4\mu_g}$
$\alpha=5.32; \beta=37.2$	$10 < Re_\omega \leq 20$	(Dennis <i>et al.</i> 1980)
$\alpha=6.44; \beta=32.2$	$20 < Re_\omega \leq 50$	
$\alpha=6.45; \beta=32.1$	$Re_\omega \geq 50$	

For the integration of Eq. (1) as well as Eq. (8) a simple explicit first order scheme was used to update the velocities and positions of the particles.

Inlet and outlet conditions

In the riser section of a CFB there is a continuous throughflow of particles which has to be accounted for in the simulation. Instead of simulating the entire riser section, including inlet and exit configurations, only the middle section was simulated. At the inlet of the simulated system particles were placed at random in the bottom row of cells ensuring no overlap with other particles or walls. An initial axial velocity was assigned to each particle fed to the system. At each time step a specific number of particles was fed to the riser duct in accordance with a specified solids mass flux. The cross sectional area in this (two-dimensional) case was assumed to be equal to the width of the system times the particle diameter. At the outlet particles which had crossed the upper boundary were simply removed from the system at each time step.

Gas Phase Hydrodynamics

The motion of the gas-phase is calculated from the following set of equations, which can be seen as a generalized form of the spatially averaged Navier-Stokes equations for a two-phase gas-solid mixture (Kuipers *et al.* (1992)).

Continuity equation gas phase:

$$\frac{\partial(\varepsilon \rho_g)}{\partial t} + (\nabla \cdot \varepsilon \rho_g \mathbf{u}) = 0 \cdot \quad (9)$$

Momentum equation gas phase:

$$\frac{\partial(\varepsilon\rho_g \mathbf{u})}{\partial t} + (\nabla \cdot \varepsilon\rho_g \mathbf{u}\mathbf{u}) = -\varepsilon\nabla p - \mathbf{S}_p - (\nabla \cdot \varepsilon\boldsymbol{\tau}_g) + \varepsilon\rho_g \mathbf{g} \quad (10)$$

In this work transient, two-dimensional, isothermal ($T = 293$ K) flow of air at slightly elevated pressure ($p = 1.2$ Bar) is considered. The constitutive equations and the boundary conditions used can be found in Hoomans *et al.* (1996). Note that no turbulence modeling is included in our present description. The void fraction (ε) is calculated from the particle positions in the bed. There is one important modification with respect to our previous model and that deals with the way in which the two-way coupling between the gas-phase and the particle motion is established. In the present model the reaction forces to the forces exerted on a particle by the gas-phase per unit of volume is fed back through the source term \mathbf{S}_p [Nm^{-3}]. A more detailed discussion on this approach can be found in Delnoij *et al.* (1997).

Results

As a first test case for our model we chose the same system as was used by Tsuo and Gidaspow (1990) and Tanaka *et al.* (1996) in their simulations. The general parameter settings are summarized in Table 2.

Table 2, General parameter settings

Particles		System		Gas	
Diameter	500 μm	Width	0.08 m	Temperature	293 K
Density	2620 kg/m^3	Height	2.00 m	Pressure	1.2 Bar
Mass flux	25 $\text{kg}/\text{m}^2\text{s}$			Velocity	5.0 m/s

The simulations were run for 20 seconds real time using a time step of 10^{-4} s. This rather long simulation time was necessary in order to allow the system to become stationary and to have sufficient data to obtain statistically reliable time averages.

Effect of collision parameters

At first the influence of the collision parameters was examined. Tanaka *et al.* (1996) reported a strong dependency of the flow structure with respect to the coefficients of restitution (e) and friction (μ). In our previous work on bubbling and slugging fluidized beds (Hoomans *et al.*, 1996) these parameters also turned out to be of have a decisive influence on the flow behavior. We performed three different simulations where the collision parameters were set according to the values presented in Table 3.

Table 3, Parameter settings for the simulations with different collision parameters

	e	μ	e_{wall}	μ_{wall}
Ideal	1.0	0.0	1.0	0.0
Non-ideal	0.94	0.28	0.94	0.28
Ideal particles/ non-ideal walls	1.0	0.0	0.94	0.28

Two typical snapshots of simulations with ideal ($e = 1$, $\mu = 0$ for both particle-particle and particle-wall collisions) and non-ideal ($e = 0.94$ and $\mu = 0.28$) collision parameters are shown in Fig. (1).

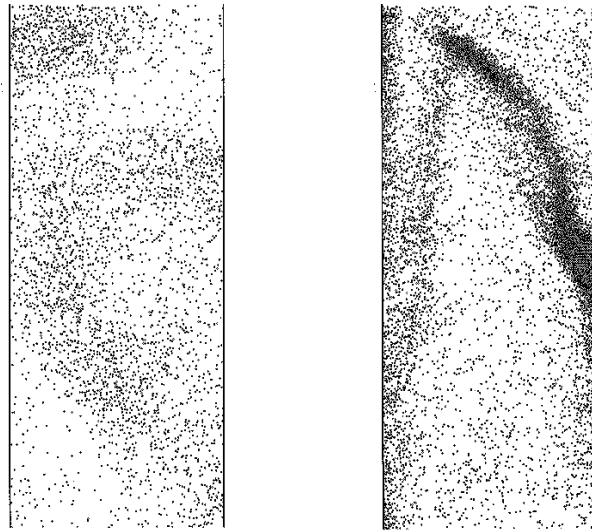


Figure 1, Snapshots of a small section of the simulated riser (width = 0.08 m). Left: ideal collision parameters, $e = 1$, $\mu = 0$, Right: non-ideal collision parameters: $e = 0.94$, $\mu = 0.28$.

It can be clearly observed that in the case of non-ideal collision parameters clusters were formed. These clusters moved downward preferably along the walls and had a streaky, semi-parabolic shape. These clusters are rather dynamic in nature: they continuously form, grow and eventually break up. Typical downward velocities for these clusters are in the order of magnitude of 1.0 m/s which is in agreement with the experimental findings of Tsuo and Gidaspow (1990). In the case of ideal collision parameters the flow was much more homogeneous and although locally slightly denser regions can be distinguished, these can hardly be typified as being clusters. Similar results were obtained in a simulation with ideal collision parameters for particle-particle collisions but non-ideal parameters for particle-wall collisions.

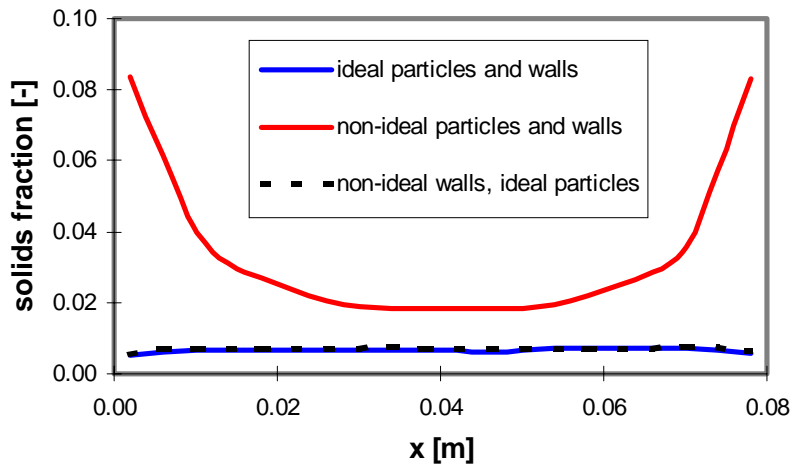


Figure 2, Radial profile of the time-averaged solids volume fraction at 0.2 [m] above the inlet of the simulated riser.

In Fig. (2) the time-averaged radial distribution of the solids volume fraction at 0.2 m above the riser inlet are presented for the three cases mentioned above. The averages are taken over the final 10 seconds of the simulations. For the complete non-ideal case the typical core-annulus structure can be observed whereas for the other two cases the radial profile is flat. This finding is a strong indication that the formation of clusters, which is clearly present in

the non-ideal case, causes the typical core-annulus structure because no cluster formation was observed in the other two cases.

Effect of superficial gas velocity

The effect of the superficial gas velocity (u_{gas}) was investigated for the non-ideal case. Simulations were performed with u_{gas} equal to 5.0, 7.5 and 10.0 m/s. Time averaged radial solids profiles at 0.2 m above the inlet are presented in Fig. (3).

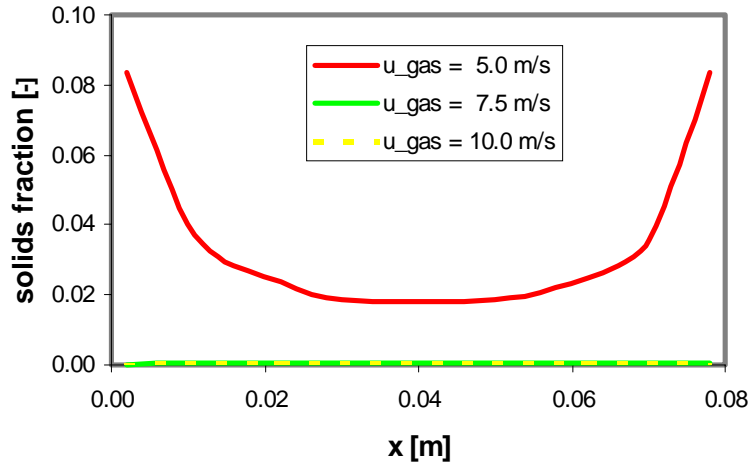


Figure 3, Influence of the superficial gas velocity on the time-averaged radial distribution of the solids volume fraction at 0.2 m above the inlet of the simulated riser.

The core-annulus flow structure in the case of $u_{\text{gas}} = 5.0$ m/s disappears completely when u_{gas} is increased to 7.5 m/s. The results for $u_{\text{gas}} = 10.0$ m/s are very similar to the results with $u_{\text{gas}} = 7.5$ m/s. Snapshots of the latter simulations were rather similar to the snapshot for the ideal case presented on the left in Fig. (1): hardly any clustering could be observed. It is also apparent from Fig. (3) that the solids fraction is far lower in the case of the higher gas velocities indicating a build up of an axial solids profile in the axial direction in the case of $u_{\text{gas}} = 5.0$ m/s.

Influence of lift forces

By default the two lift forces in Eq. (1) were not included in the simulations. However one simulation was performed including these lift forces in order to investigate their influence on the flow structure. The non-ideal case with a superficial gas velocity of 5.0 m/s was used as a test case. The time-averaged radial distribution of the solids volume fraction at 0.2 m above the riser inlet are presented in Fig. (4) for the two simulations.

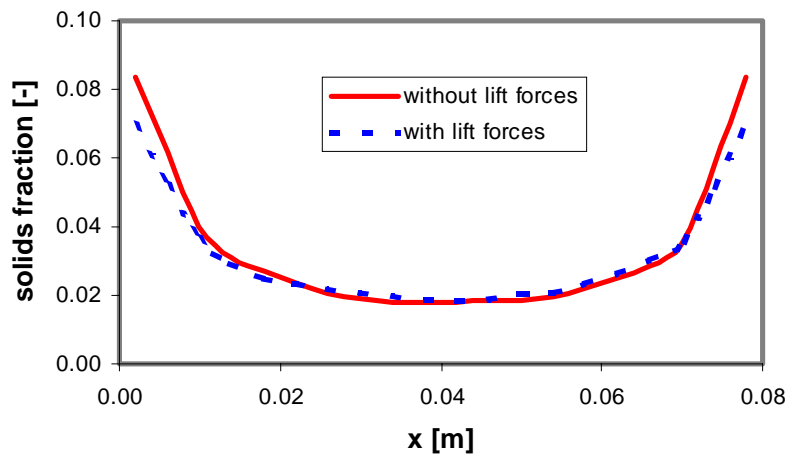


Figure 4, Influence of the lift forces on the time-averaged radial distribution of the solids volume fraction at 0.2 m above the inlet of the simulated riser.

From Fig. (4) it is apparent that the lift forces did not have a significant influence on the flow structure. The radial segregation is slightly less pronounced when the lift forces are included in the equation of motion. This can be understood since the lift forces tend to move the particles toward the center of the riser and have therefore a dispersive effect.

Discussion and Conclusions

Granular Dynamics simulations of riser flow have been performed using a two-dimensional hard-sphere discrete particle model. Particles of 500 μm diameter and a density of 2620 kg/m^3 were introduced in a riser of 0.08 m width and 2.00 m height at a solids mass flux of 25 $\text{kg/m}^2\text{s}$. By default the superficial gas velocity was set equal to 5.0 m/s. The simulations turned out to be rather sensitive to the collision parameters, i.e. the coefficients of restitution (e) and friction (μ). When these parameters were assigned non-ideal values ($e = 0.94$, $\mu = 0.28$) cluster formation was observed. The time-averaged radial distribution of the solids volume fraction clearly revealed the typical core-annulus structure. When the collision parameters were set to ideal values ($e = 1$, $\mu = 0$) no cluster formation was observed. This was also the case in a simulation where only particle-wall collisions were considered non-ideal whereas particle-particle collisions were still taken to be ideal. Time averages of the radial solids fraction did not show the typical core-annulus structure. Simulations at higher superficial gas velocities for the case where non-ideal collision parameters were used showed that already at a velocity of 7.5 m/s cluster formation did not occur and hence no core-annulus structure was found. Similar behavior was observed in the simulation where the superficial gas velocity was set equal to 10.0 m/s. Finally the influence of the lift forces was investigated. These forces turned out to have a slightly redispersive effect on the flow structure which made the radial segregation of the solids a little less pronounced. Since this was only a minor effect it could be regarded as a justification for the fact that the lift forces were neglected in the default simulations.

Acknowledgment

P.W. Schinkelshoek is gratefully acknowledged for his contribution to the development of the computer code.

List of Symbols

C_d	drag coefficient, [-]	<i>Greek symbols</i>	
e	coefficient of restitution, [-]	χ	velocity gradient, [1/s]
d_p	particle diameter, [m]	ε	void fraction, [-]
\mathbf{g}	gravitational acceleration, [m/s^2]	μ	coefficient of friction, [-]
m_p	particle mass, [kg]	μ_g	gas viscosity, [kg/ms]
p	pressure, [Pa]	$\boldsymbol{\tau}$	gas-phase stress tensor, [kg/ms^2]
\mathbf{r}	position vector, [m]	ρ_g	gas density, [kg/m^3]
\mathbf{S}_p	momentum source term Eq. (10), [N/m^3]	ω	particle rotational velocity [1/s]
t	time, [s]	ξ	dimensionless velocity gradient, [-]
\mathbf{u}	gas velocity vector, [m/s]		
\mathbf{v}_p	particle velocity vector, [m/s]		

References

- Delnoij, E., Lammers, F.A., Kuipers, J.A.M. and van Swaaij, W.P.M., 1997, "Dynamic simulation of dispersed gas-liquid two-phase flow using a discrete bubble model," *Chem. Engng Sci.*, **52**, 1429.
- Dennis, S.C.R., Singh, S.N., Ingham, D.B., 1980, "The steady flow due to a rotating particle at low and moderate Reynolds numbers," *J. Fluid Mech.*, **101** (2), 257.
- Frezzotti, A., 1997, "A particle scheme for the numerical solution of the Enskog equation", *Phys. Fluids*, **9** (5), 1329.

- Hrenya, C.M. and Sinclair, J., 1997, "Effects of particle phase turbulence in gas-solid flows", *AIChE J.*, **43**(4), 853.
- Hoomans, B.P.B., Kuipers, J.A.M., Briels, W.J., Van Swaaij, W.P.M., 1996, "Discrete particle simulation of bubble and slug formation in two dimensional gas-fluidised beds: A hard sphere approach", *Chem. Engng Sci.* **51**, 99-118.
- Kuipers, J.A.M., van Duin, K.J., van Beckum, F.P.H. and van Swaaij, W.P.M, 1992, "A numerical model of gas-fluidized beds," *Chem. Engng Sci.*, **47**, 1913.
- Mei, R., 1992, "An approximate expression for the shear lift force on a spherical particle at finite Reynolds number," *Int. J. Multiphase flow*, **18**, 145.
- Nieuwland, J.J., van Sint Annaland, M., Kuipers, J.A.M. and van Swaaij, W.P.M., 1996, "Hydrodynamic modelling of gas-particle flows in riser reactors", *AIChE J.*, **37**(7), 1009.
- Oesterlé, B. 1994, "Une étude de l'influence des forces transversales agissant sur les particules dans les écoulements gaz-solide," *Powder Technol.*, **79**, 81.
- Richardson, J.F. and Zaki, W.N., 1954, "Sedimentation and Fluidisation: Part I.", *Trans. Inst. Chem. Engng*, **32**, 35.
- Saffman, P.G., 1965, "The lift on a small sphere in a slow shear flow", *J. Fluid Mech.* **22**(2), 385.
- Sinclair, J. and Jackson, R., 1989, "Gas-particle flow in a vertical pipe with particle-particle interactions", *AIChE J.*, **35**(5), 1473.
- Tanaka, T., Yonemura, S., Kiribayashi, K., Tsuji, Y., 1996, "Cluster formation and particle-induced instability in gas-solid flows predicted by the DSMC method", *JSME Int. J. Series B*, **39**(2), 239-245.
- Tsuji, Y., Morikawa, Y. and Mizuno, O., 1985, "Experimental measurement of the Magnus lift force on a rotating sphere at low Reynolds numbers", *J. Fluids Eng.*, **107**, 484.
- Tsuo, Y.P. and Gidaspow, D., 1990, "Computation of flow patterns in circulating fluidized beds", *AIChE J.* **36**(6), 885.
- Wang, Y. and Mason, M.T, 1992, "Two-dimensional rigid-body collisions with friction," *J. Appl. Mech.*, **59**, 635.